Chemical route for synthesis of β-SiAlON:Eu2+ phosphors combining polymer-derived ceramics route with non-hydrolytic sol-gel chemistry

Yang Gao, Daiki Hamana, Ryo Iwasaki, Junya Iihama, Sawao Honda, Munni Kumari, Tomokatsu Hayakawa, Samuel Bernard, Philippe Thomas, Yuji Iwamoto

Journal of Sol-Gel Science and Technology
https://doi.org/10.1007/s10971-022-05879-w

INVITED PAPER: SOL-GEL, HYBRIDS AND SOLUTION CHEMISTRIES

Chemical route for synthesis of β-SiAlON:Eu^{2+} phosphors combining polymer-derived ceramics route with non-hydrolytic sol-gel chemistry

Yang Gao[1] · Daiki Hamana[1] · Ryo Iwasaki[1] · Junya Iihama[1] · Sawao Honda[1] · Munni Kumari[2] · Tomokatsu Hayakawa[1] · Samuel Bernard[2] · Philippe Thomas[2] · Yuji Iwamoto[1]

Received: 30 May 2022 / Accepted: 7 June 2022

Abstract

We report the synthesis of β-SiAlON:Eu^{2+} phosphors from novel *single source* precursors in which strictly controlled chemical composition is established at molecular scale. The two-step synthesis occurs by the chemical modification of perhydropolysilazane (PHPS) with $Al(OCH(CH_3)_2)_3$ and $AlCl_3$ in xylene at room temperature to 140 °C to introduce Al in the PHPS network while controlling the oxygen content followed by the reaction of $EuCl_2$ with the Al-modified PHPS upon heat-treatment. Gas chromatography-mass spectrometry and thermogravimetry-mass spectrometry analyses revealed that PHPS reacted with $Al(OCH(CH_3)_2)_3$ and $AlCl_3$ via the formation of Al-N bonds. Moreover, $AlCl_3$ reacted with nitrogen-bonded Al alkoxide residue to release 2-chloropropane in an analogy to the non-hydrolytic sol-gel reaction between metal alkoxide and metal chloride. Subsequently, $AlCl_3$ acted as a Lewis acid catalyst to promote the Friedel-Craft alkylation between xylene solvent and the 2-chloropropane formed in-situ to afford dimethylcumene. On the other hand, $EuCl_2$ reacted with silylamino moiety to form Eu-N bonds at around 850 °C. β-SiAlON:Eu^{2+} phosphors were successfully synthesized by pyrolysis of the precursors under flowing N_2 or NH_3 at 1000 °C, followed by heat treatment at 1800 °C for 1 h under a N_2 gas pressure at 980 kPa. The polymer-derived β-SiAlON:Eu^{2+} ($z = 0.55$, Eu^{2+} 0.37 at%) exhibited green emission under excitation at 410 or 460 nm, and the green emission intensity under the excitation at 410 nm was found to be increased by reducing the carbon and chlorine impurities through the polymer-derived ceramics route investigated in this study.

Graphical abstract

Keywords β-SiAlON · Eu(II) · Non-hydrolytic sol-gel reaction · Polymer-derived ceramics · Photoluminescence

✉ Yuji Iwamoto
iwamoto.yuji@nitech.ac.jp

[1] Department of Life Science and Applied Chemistry, Graduate School of Engineering, Nagoya Institute of Technology, Gokiso-cho, Showa-ku, Nagoya 466-8555, Japan

[2] University of Limoges, CNRS, IRCER, UMR 7315, F-87000 Limoges, France

Published online: 27 June 2022

Highlights

- β-SiAlON:Eu^{2+} phosphors were synthesized from Al- and Eu-modified perhydropolysilazanes.
- The modification using $Al(OCH(CH_3)_2)_3$ with $AlCl_3$ promoted non-hydrolytic sol-gel (NHSG) reaction.
- The NHSG reaction and NH_3-pyrolysis synergistically contributed to reducing C and Cl impurities.
- The β-SiAlON:Eu^{2+} ($z = 0.55$, Eu^{2+} 0.37 at%) exhibited green emission ($\lambda_{ex} = 410$ or 460 nm.
- The green emission intensity ($\lambda_{ex} = 410$ nm) was increased by reducing C and Cl impurities.

1 Introduction

The light-emitting diodes (LEDs) based solid-state lighting technology has been developed worldwide to replace the traditional illumination sources to save energy and reduce the cost. Phosphor is one of the most important materials in this solution [1], and the phosphor-converted white LEDs have attracted much attention. Currently, the blue LED-driven white LEDs have been produced by blending the blue-emitting LED chips with a yellow phosphor or a green-emitting phosphor together with a red-emitting phosphor (two-pc wLEDs).

Eu^{2+} activated β-SiAlON (β-SiAlON:Eu^{2+}) is a kind of green-emitting phosphor that has been reported widely [2–6] and successfully utilized for the two-pc wLEDs. The general formula of β-SiAlON can be expressed as $Si_{6-z}Al_zO_zN_{8-z}$, in which the z value respects the Al concentration in the system. Wang et al. put forward a modified formula, $Si_{6-z}Al_zO_{z-2y}N_{8-z+2y}$:$yEu^{2+}$, where the charge compensation for the introduced Eu^{2+} ions are taken into account [3]. β-SiAlON:Eu^{2+} phosphors have been manufactured by the conventional powder metallurgy method using α-Si_3N_4, α-alumina (Al_2O_3), and aluminum nitride (AlN) as starting powder materials. The general fabrication conditions of high-temperature heat treatment at $T \geq 1800$ °C under a high nitrogen pressure at $P \geq 0.98$ MPa are required to afford β-SiAlON as a thermodynamically favorable phase [4, 5].

Ceramic processing methods based on the molecular chemistry of organometallic precursors are efficient approaches to synthesizing such high-performance functional ceramics with accurately-controlled chemical composition along with the local structure at the molecular size scale level [7–13]. Among them, the polymer-derived ceramics (PDCs) route is convenient and appropriate for the synthesis of silicon (Si)-based non-oxide ceramic systems [11–13]. In this route, polysilazane derivatives are frequently used as a starting polymer precursor, especially perhydropolysilazane (PHPS) composed of only Si, N, and H elements has some advantages in high purity and high ceramic yield for Si_3N_4 ceramics synthesis [14–16]. Moreover, PHPS is highly reactive and easily modified with various monomeric organometallic compounds including metal alkoxides ($M(OR)_x$, M = B [17], Al [18, 19], Y [20–23]), metal chlorides (MCl_n, M = Ti [23], Co [24], Ni [25]) and metal amides ($M(NR_2)_x$, M = Ti [26–28], B [29]). The resulting multicomponent polymers have been successfully converted to polycrystalline Si_3N_4-based composites such as silicon carbide (SiC) [21, 22] or titanium nitride (TiN) [23, 26–28] nanoparticle-dispersed Si_3N_4, pseudo-binary Si_3N_4-Y_2O_3 [20] and SiAlONs [18, 19].

Recently, we have succeeded in the synthesis of β-SiAlON:Eu^{2+} phosphors through the PDCs route for the first time: *single source* precursors were synthesized by chemical modification of PHPS ($(SiH_2\text{-}NH)_n$) with aluminum triisopropoxide ($Al(OCH(CH_3)_2)_3$), and europium (II) chloride ($EuCl_2$), then converted to β-SiAlON:Eu^{2+} phosphors by pyrolysis under flowing N_2 at 1000 °C followed by heat treatment at 1800 °C under a N_2 gas pressure at 980 kPa [19]. Based on the PDCs route, in-situ formation of β-SiAlON from the *single source* precursor-derived multicomponent amorphous compound has been recognized to proceed by the nucleation and crystallization of α-SiAlON and subsequent α-/β-phase transformation promoted by the dissolution, diffusion and re-precipitation processes through the Si-Al-Eu-O-N transient liquid phase formed in-situ [19]. The amount of the transient liquid phase increases consistently with the Al and O contents i.e. the Al/Si ratio in the *single source* precursor synthesis, and the minimum Al/Si ratio in the precursor synthesis for completing α-/β-phase transformation of the polymer-derived host SiAlON was found as 0.09 [19]. Moreover, the critical Eu/Si atomic ratio in terms of the β-SiAlON single phase formation without impurity phases including SiAlON polytypoids was found as 0.05, and the resulting Eu^{2+} critical concentration for the polymer-derived β-SiAlON ($z = 0.55$) reached 1.48 at% [19], which was approximately three times higher than the reported value (0.5 at%) suggested for the β-SiAlON ($z = 0.5$) fabricated through the conventional powder metallurgy route [4]. However, our previous PDCs route limited the amount of $Al(OCH(CH_3)_2)_3$ to avoid the formation of impurity phases such as oxygen-rich J-SiAlON and mullite ($3Al_2O_3$-$2SiO_2$) phases due to the excess oxygen introduced from the Al alkoxide modifier with the O/Al ratio of 3 [18].

In this study, $Al(OCH(CH_3)_2)_3$ was partly replaced with aluminum trichloride ($AlCl_3$). It is expected to introduce Al to PHPS network independently with oxygen content: *single source* polymeric precursors were synthesized by chemical modification of a commercially available PHPS with $Al(OCH(CH_3)_2)_3$, $AlCl_3$, and $EuCl_2$, then converted to Eu^{2+}-doped amorphous SiAlON by pyrolysis at 1000 °C under flowing N_2

Table 1 Nominal molar ratios for the synthesis of *single source* precursors for β-SiAlON:Eu^{2+}

Name	Si in $[SiH_2\text{-}NH]_n$ (PHPS)	M/Si ratio			Calculated chemical composition					
					Formula	$Si_{6-z}Al_zO_{z-2y+\delta}N_{8-z+2y+\gamma}$: yEu^{2+}				Eu^{2+} (at%)
		$Al(OCH(CH_3)_2)_3$	$AlCl_3$	$EuCl_2$		z	y	δ	γ	
A90E1 [19]	1	0.09	0.00	0.01	$SiAl_{0.09}O_{0.27}N_{1.00}Eu_{0.01}$	0.50	0.055	1.10	−2.11	0.42
A63E1	1	0.06	0.03	0.01	$SiAl_{0.09}O_{0.18}N_{1.00}Eu_{0.01}$	0.50	0.055	0.61	−2.11	0.44
A36E1	1	0.03	0.06	0.01	$SiAl_{0.09}O_{0.09}N_{1.00}Eu_{0.01}$	0.50	0.055	0.11	−2.11	0.46

or NH_3. Subsequently, the polymer-derived multicomponent amorphous compounds were converted to β-SiAlON:Eu^{2+} phosphors by heat treatment at 1800 °C for 1 h under a N_2 gas pressure at 980 kPa. The chemical reactions during precursor synthesis and subsequent pyrolysis were monitored by infrared spectroscopy, simultaneous gas chromatography-mass spectrometry (GC-MS) analyses as well as thermogravimetry-mass spectrometry (TG-MS) analyses. Photoluminescence (PL) properties of the polymer-derived β-SiAlON:Eu^{2+} phosphors were discussed based on a set of characterization techniques including elemental analysis, X-ray diffraction (XRD), PL spectroscopy and a scanning electron microscope (SEM) observations.

2 Experimental procedures

2.1 Materials and methods

Commercial PHPS (AZ NN110-20, 20 wt% xylene solution, AZ Electronic Materials Co., Ltd., Tokyo, Japan), $Al(OCH(CH_3)_2)_3$ (99.9%, Kojundo Chemical Laboratory Co. Ltd., Saitama, Japan), $AlCl_3$ (99.9 %, Sigma-Aldrich Japan, Tokyo, Japan) and $EuCl_2$ (99.9 %, Sigma-Aldrich Japan, Tokyo, Japan) were used as-received. The handling of the chemicals and reagents was performed under a dry argon (Ar) atmosphere using standard Schlenk techniques.

Single source precursor syntheses were conducted according to parameters and calculated compositions listed in Table 1. Al/Si atomic ratio for the chemical modification of PHPS was fixed as 0.09 based on our previous result [19] and the resulting z value of the polymer-derived host β-SiAlON was calculated as 0.5 by the theoretical β-SiAlON formula, $Si_{6-z}Al_zO_{z-2y}N_{8-z+2y}$:$yEu^{2+}$ given by Wang et al. [3]. In addition, $Al(OCH(CH_3)_2)_3$ was partially replaced by $AlCl_3$ to try to control the oxygen content independently with total Al content. The resulting nominal chemical composition was expressed by the modified formula, $Si_{6-z}Al_zO_{z-2y+\delta}N_{8-z+2+\gamma}$:$yEu^{2+}$. The values of the δ and γ were also listed in this table. We targeted pyrolysis and subsequent heat treatment of the *single source* precursor to afford the appropriate composition of β-SiAlON:Eu^{2+} phosphor via several reactions such as carbothermal reduction and nitridation. On the other hand, the Eu/Si ratio was fixed as 0.01 so as to control the Eu^{2+} cation concentration in the β-SiAlON as 0.42–0.46 at%, lower than the critical Eu^{2+} concentration (0.5 at%) previously suggest for the β-SiAlON with $z = 0.5$ [4].

Here, we describe the synthesis of the AE63E1 sample, which is well representative of the synthesis process applied to all the samples. In a typical experiment, A 300 mL two-neck round-bottom flask equipped with a magnetic stirrer was charged with PHPS (Si: 67.91 wt%, 10 mL of 20 wt% xylene solution, i.e. Si 48.4 mmol), $Al(OCH(CH_3)_2)_3$ (0.593 g, 2.90 mmol), $AlCl_3$ (0.193 g, 1.45 mmol) and $EuCl_2$ (0.108 g, 0.48 mmol), then refluxed for 1 h. After the reaction mixture was cooled down to room temperature (RT), the solvent was removed under vacuum at RT. The residue of the white solid precursor was subsequently pyrolyzed in a tube furnace (model ARF60–150–31KC, Asahi Rika, Chiba, Japan) under flowing N_2 or NH_3 at 1000 °C for 1 h with a heating rate of 5 °C min^{-1}. Then, the pyrolyzed powder was heat-treated in a graphite resistance-heated furnace (model High Multi 5000, Fujidempa Kogyo, Co., Ltd., Osaka, Japan) at 1800 °C for 1 h under a N_2 gas pressure at 980 kPa.

2.2 Characterizations

The chemical modification reactions of PHPS were monitored by attenuated total reflection Flourier transform infrared (ATR-FTIR) spectroscopy using a FTIR spectrometer (model FT/IR-4200IF, JASCO Corporation, Tokyo, Japan) attached with an ATR equipment (model ATR PRO 550S-S/570S-H, JASCO Corporation, Tokyo, Japan) at a resolution of 4 cm^{-1}.

The detail of the chemical reactions during the precursor synthesis from RT to 140 °C (xylene reflux) and precursor pyrolysis up to 1000 °C were monitored by GC-MS and TG-MS analyses under He flow, respectively (model STA7200, Hitachi, Tokyo, Japan). Commercially available 2-propanol (≥99%, Sigma-Aldrich Japan, Tokyo, Japan) and 3,5-dimethyl-1-isopropylbenzene (dimethyl cumene, ≥ 80 %, Tokyo Chemical Industry Co., Ltd., Tokyo, Japan) were used as references for the GC-MS analyses.

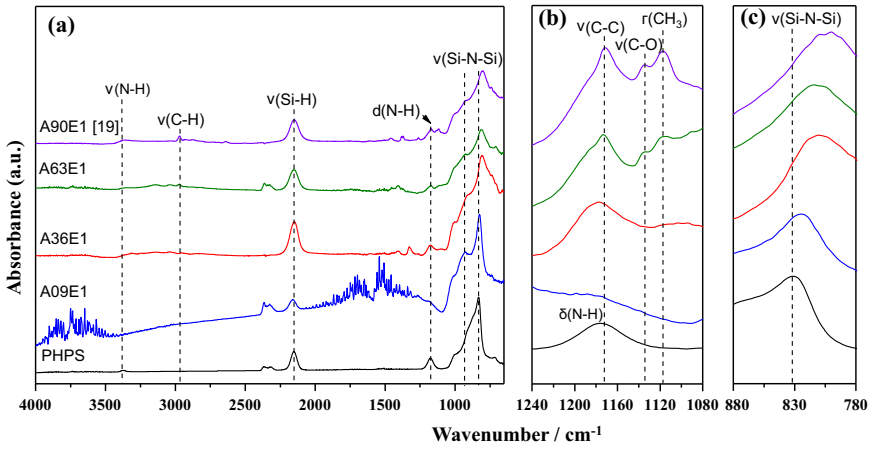

Fig. 1 ATR-IR spectra for as-received PHPS and Al, Eu-modified PHPSs: **a** 4000–600 cm^{-1}, **b** 1240–1080 cm^{-1}, **c** 880–780 cm^{-1}

XRD analysis for the heat-treated samples was performed (model X' Pert-Pro α1, PANalytical, UK) using a Cu k-alpha radiation. The β phase ratio of the polymer-derived SiAlON-based samples was defined as the $\beta/(\beta+\alpha)$ phase ratio evaluated by comparing the diffraction peak intensity (I) of the α-phase (102), (210) plane and that of β-phase (101), (210) plane as follows [19, 30]:

$$\beta\text{-phase ratio} = (I\beta(101) + I\beta(210))/[(I\beta(101) + I\beta(210)) + (I\alpha(102) + I\alpha(210))] \times 100 \quad (1)$$

Elemental analyses for oxygen (O), nitrogen (N) by the inert-gas fusion method (model EMGA-930, Horiba, Kyoto, Japan) and carbon (C) by the non-dispersive infrared method (model CS844, LECO CORPORATION, St. Joseph, USA) were performed on the 1000 °C-pyrolyzed and subsequent 1800 °C-heat-treated samples. The Al and Eu contents in the polymer-derived SiAlON:Eu^{2+} samples were analyzed by using an energy dispersive X-ray spectrometer (EDS) mounted on a SEM (model JSM-6010LA, JEOL Ltd., Tokyo, Japan). In this study, EDS element mapping analysis was performed on the powdered sample surfaces observed within a SEM image area of approximately 20×25 (μm^2) at the magnification and accelerating voltage of 5000x and 15 kV, respectively to give an atomic percentage for all the constituent elements. For each sample, the Al/Si and Eu/Si ratios were evaluated as an average value of the mapping scans conducted for at least five different areas randomly selected. Then, the chemical composition of the polymer-derived SiAlON-based samples was determined as follows [19]:

$$wt\%(Si + Al + Eu) = 100\% - wt\%(C) - wt\%(N) - wt\%(O) \quad (2)$$

Morphology of the polymer-derived β-SiAlON:Eu^{2+} samples was observed by using a SEM (model JSM-6010LA, JEOL Ltd., Tokyo, Japan). The PL emission and excitation spectra were recorded at RT using a fluorescence spectrometer (model F-7000, Hitachi, Tokyo, Japan) with a xenon (Xe) lamp.

3 Results and discussion

3.1 Precursor synthesis

The ATR-IR spectra of polymer samples are shown in Fig. 1(a). As received PHPS exhibits characteristic absorption peaks at 3400 (νN-H), 2152 (νSi-H), 1175 (δN-H) and 832 (νSi-N-Si) cm^{-1} [14–16]. In addition to these peaks, the modified samples exhibit new peaks at 2900 cm^{-1} assigned to νC-H, 1172, 1135 and 1118 cm^{-1} assigned to νC-C, νC-O and rCH_3 of isopropyl ($-OCH(CH_3)_2$) group [31], respectively (Fig. 1(b)), meanwhile the Si-N-Si broad peak centered at 832 cm^{-1} shows an obvious red shift, especially in the spectra of **A90E1** and **A63E1** synthesized by using the higher amount of $Al(OCH_2(CH_3)_2)_3$ at the Al/Si ratio ≥0.06 (Fig. 1(c)). The highest degree of the peak shift in these spectra is possibly due to the mass effect on stretching frequencies, i.e., $Al(OCH(CH_3)_2)_3$ reacted with NH groups in PHPS to form N-Al bonds [18, 19], and the substitution of $Al(OCH(CH_3)_2)_{3-x}$ for H lead to the red shift of the Si-N-Si peak:

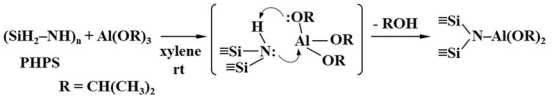

(3)

A36E1 sample, which was synthesized by using higher

amount of $AlCl_3$ also shows slight red shift of the Si-N-Si peak (Fig. 1(c)). To investigate the peak shift in more detail, **A09E1** sample was synthesized by modification of PHPS with $AlCl_3$ at the Al/Si ratio of 0.09. As shown in Fig. 1(c), **A09E1** shows an apparent red shift of the Si-N-Si peak. These changes in the ATR-IR spectra reveal the formation of a typical Lewis acid-base adduct via the coordination of the lone pair of =NH in ≡Si-NH-Si≡ to $AlCl_3$ as previously suggested for chemical modification of PHPS with cobalt (II) chloride ($CoCl_2$) [24] and $NiCl_2$ [25]. In addition, the peak intensity at 920 cm^{-1} (observed on the left shoulder of the broad peak attributed to νSi-N-Si) increases consistently with the amount of $AlCl_3$ used for the chemical modification of PHPS (**A36E1** and **A09E1** in Fig. 1(a)). This band is attributed to νSi-N-Si of low molecular components [32], which suggests that partial cleavage of Si–N bonds or bond redistribution reaction such as trans-amination reaction proceeded in the presence of Lewis acid $AlCl_3$ during xylene refluxing at 140 °C.

As we reported previously [19], under the present synthesis condition, $EuCl_2$ remained unchanged and began to react with PHPS-derived silylamino moieties to form Eu-N bonds above 600 °C. In addition, the present chemical modification with $EuCl_2$ was performed at the Eu/Si ratio of 0.01, and thus it was difficult to identify the existence of $EuCl_2$ clearly by the ATR-IR spectroscopic analysis. Then, chemical reactions during the precursor synthesis were ex-situ monitored by the GC-MS analyses. The results obtained for the **A36E1** sample synthesis were summarized and shown in Fig. 2. In this study, a vapor sample was taken from the reaction solution for synthesizing the **A63E1** sample at temperatures ranging from 25 to 140 °C. The chromatogram peak at 64.19 s (**I**) is due to background (mass fragments of the m/z ratios of 40 and 20 assigned to Ar applied as an inert reaction atmosphere, 32 and 28 due to O_2 and N_2, respectively). At 25 and 73 °C, the sample exhibited a new peak at 65.61 s (**II**) as well as two distinct peaks at 87.88 s (**III**) and 90.64 s (**IV**) (Fig. 2(a, b)). The peak **II** was identified as 2-propanol by detecting mass fragments at the m/z ratios of 59 ($C_3H_7O^+$), 45 ($C_2H_5O^+$), 43 ($C_3H_7^+$) and 27 ($C_2H_3^+$) [33], which revealed that Al $(OCH_2(CH_3)_2)_3$ easily reacted with PHPS at RT [19] (eq. (3)). The two distinct peaks **III** and **IV** were identified as xylene used as reaction solvent by detecting typical mass fragments at the m/z ratios of 106, 91, 77, 65, 51, 39 and 27, and suggested to be assigned to m- and p-xylene, respectively [33].

At 108 °C, additional two peaks appeared at 66.13 s (**V**) and 163.51 s (**VI**), then at 140 °C, the peak **V** decreased in intensity, while the peak **VI** conversely increased in intensity (Fig. 2(c, d)). MS analyses for the peak **V** resulted in the detection of fragment species at the m/z ratios of 78 ($(CH_3)_2CHCl^{35}$), 63 ($^+CH_2CH_2Cl^{35}$), 43 ($CH_3{}^+CHCH_3$), 27 ($CH_2=CH^+$), and 15 ($CH_3{}^+$), which were identical to those of the reference sample, 2-chloropropane ($(CH_3)_2CHCl$, Fig. 2(e)). On the other hand, the mass fragments for the peak **VI** were detected at the m/z ratios of 148 ($C_{11}H_{16}$), 133 ($C_{10}H_{13}{}^+$), 117 ($C_9H_9{}^+$), 105 ($C_8H_9{}^+$), 91 ($C_7H_7{}^+$), 77 ($C_6H_5{}^+$), 65 ($C_5H_5{}^+$), 39 ($C_3H_3{}^+$) and 27 ($C_2H_3{}^+$), which were identical to those of another reference sample, dimethylcumene ($(H_3C)_2C_6H_3$-$CH(CH_3)_2$) (Fig. 2(f)). It should be noted that, at 140 °C, an unknown minor peak appeared at 72.23 s, which was thought to be attributed to thermally decomposed species derived from PHPS (Fig. 2(d)).

The new fragments detected for the peak **V** reveal that reaction of $(\equiv Si)_2N)_xAl(OR)_{3-x}$ with $AlCl_3$ proceeded (ex. x = 1) as follows,

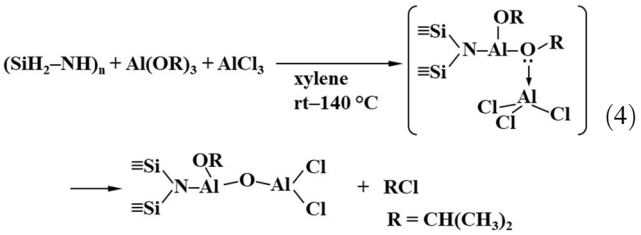

(4)

This reaction is analogous to the well-known non-hydrolytic sol-gel (NHSG) reaction reported as the homo condensation of $M(OR)_n$ and MCl_n, which generally proceeds at 80–150 °C (ex. $Al(OR)_3$ with $AlCl_3$, path (*b*)) [34–36].

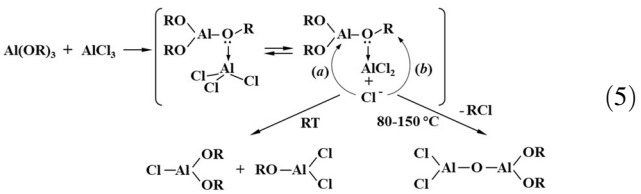

(5)

Subsequently, formation of dimethylcumene proceeded via the Friedel-Craft alkylation (FCA) between the xylene solvent ($C_6H_4(CH_3)_2$) and $(CH_3)_2CHCl$ formed in-situ (eq. (5)) in the presence of $AlCl_3$ as a Lewis acid catalyst [37].

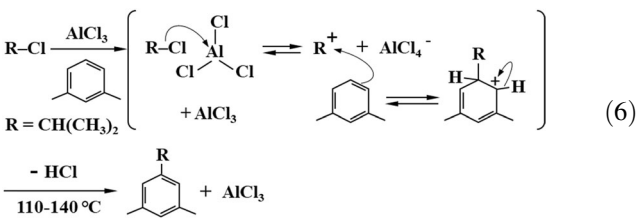

(6)

3.2 Conversion into inorganic compounds

Thermal conversion of polymers to inorganic compounds up to 1000 °C was monitored by the TG-MS analysis. The results obtained for the **A63E1** and **A36E1** samples

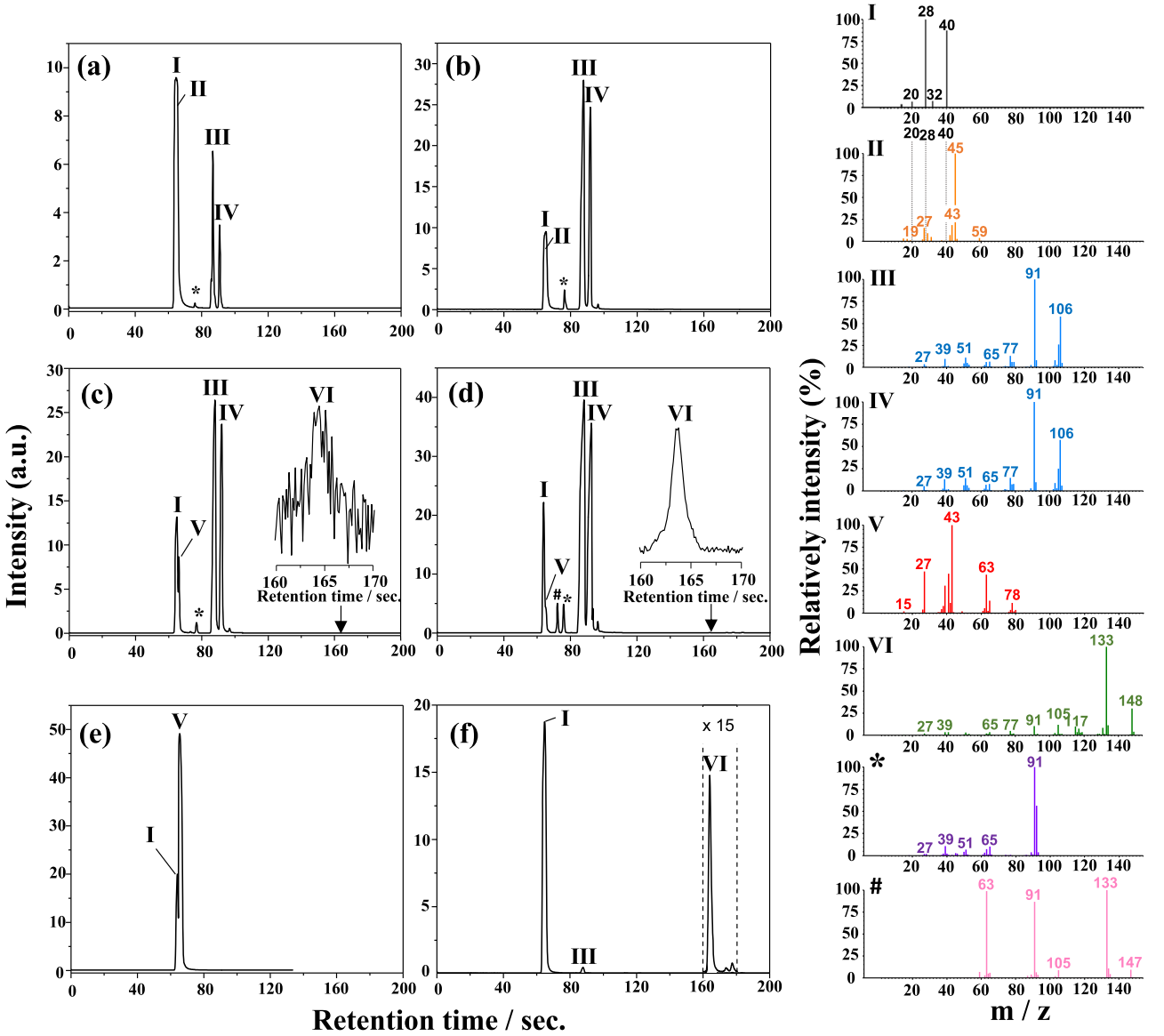

Fig. 2 Results of GC-MS analyses for ex-situ monitoring the chemical modification reactions of PHPS with $Al(OCH(CH_3)_2)_3$ and $AlCl_3$: sampling and analyses of the gaseous species evolved from the reaction solution for synthesis of **A63E1** sample performed at (**a**) 25 °C, **b** 73 °C, **c** 108 °C, **d** 141 °C (*: toluene used to clean sampling syringe). The results of the reference samples of 2-chloropropane and dimethyl cumene m-xylene solution were shown in (**e**) and (**f**), respectively

were compared with those of **A90E1** [19] and shown in Fig. 3. As shown in Fig. 3(A), the **A90E1** sample showed a total weight loss of 17 %, while the total ion current chromatogram (TICC) exhibited two distinct peaks centred at 140 and 230 °C and one minor peak around 850 °C. The results of MS analysis revealed that the first TICC peak at 140 °C was primarily attributed to the volatilization of residual xylene solvent (m/z = 106, 91, 77, 65, 63, 51, 39, and 27), while those at 133 ($Si_3N_3H_7^+$: N-SiH_2-NH-SiH_2-NH-SiH^+), 75 (H_2Si-NH-SiH_2^+), 45 (H_2Si-NH^+) and 16 (NH_2^+) could be due to the thermal decomposition of oligomers originally existed as a low molecular weight fraction of starting PHPS or formed in-situ via the partial cleavage of the -SiH_2-NH-SiH_2- linkages previously observed for the chemical modification of PHPS with other metal alkoxides [17, 19, 21].

The mass spectrum recorded at 230 °C showed three main fragments at the m/z ratios of 41 (H_3C-CH = CH^+), 29 ($CH_3CH_2^+$) and 16 (CH_4^+), thus the second TICC peak was due mainly to the thermal decomposition of the residual isopropoxy ($OCH(CH_3)_2$) group originated from $Al(OCH(CH_3)_2)_3$.

As shown in Fig. 3B, C, total weight loss up to 400 °C increased consistently with the amount of $AlCl_3$ used for the

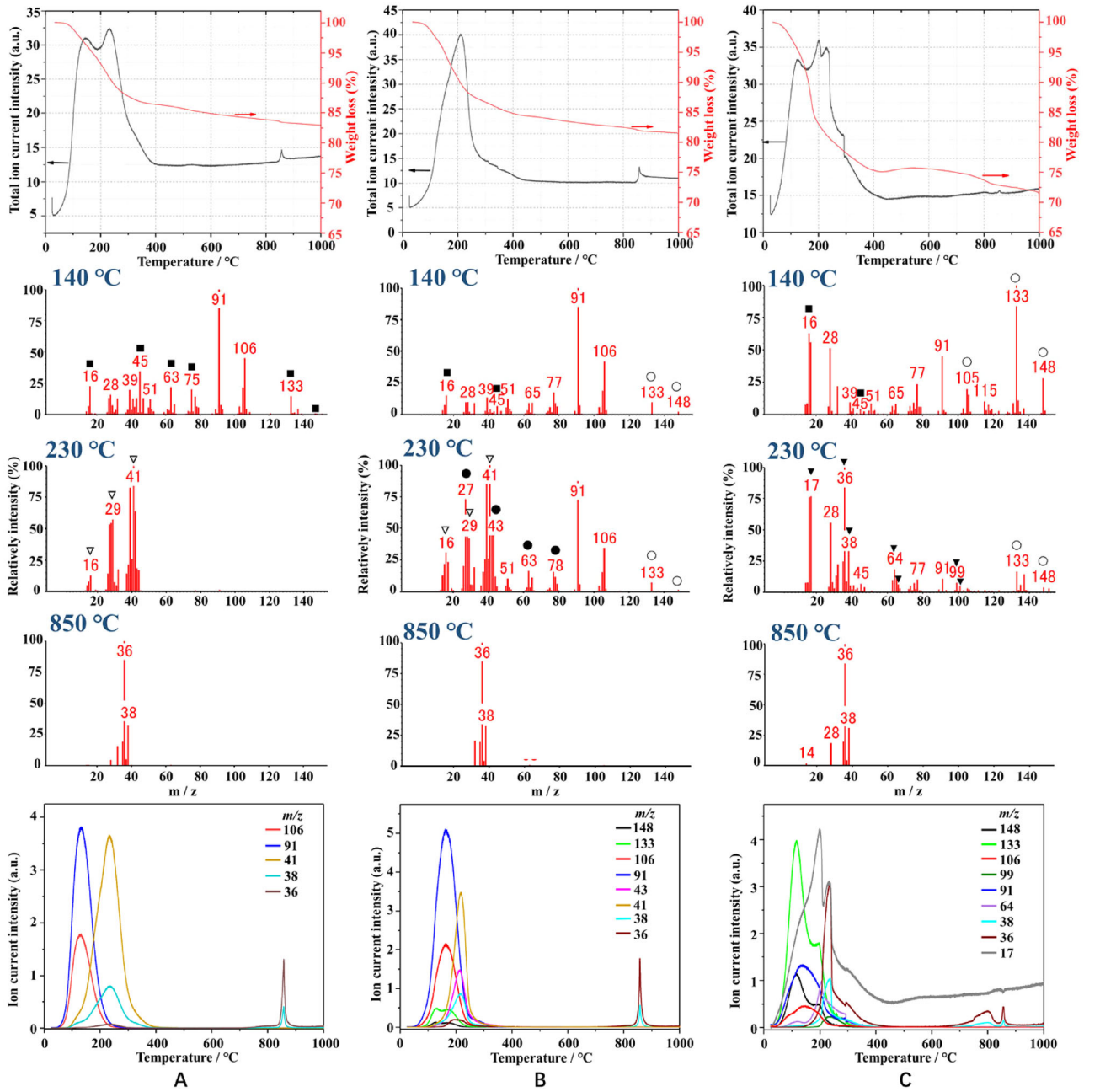

Fig. 3 Thermal behavior under He flow of Al, Eu-modified PHPS samples, **A A90E1** [19], **B A63E1**, **C A36E1**: (a) TG curve and total ion current chromatogram (TICC), (b) mass fragments monitored by mass spectrometry at specific temperatures of 140, 230, and 850 °C and (c) selected mass fragments monitored continuously during the measurement

chemical modification of PHPS and was measured to be 18 % for the **A63E1** sample (modification with $AlCl_3$ at Al/Si= 0.03) and 28 % for the **A36E1** sample (modification with $AlCl_3$ at Al/Si= 0.06). The mass spectra of these samples recorded at 140 and 230 °C showed new fragments (Fig. 3B, C): from 140 to 230 °C, the **A63E1** sample apparently increased the relative intensity at the m/z ratios = 78, 63, 43, and 27 (marked by ● in Fig. 3B) assigned as $^{35}ClCH(CH_3)_2^+$, $^{35}ClCHCH_3^+$, $CH(CH_3)_2^+$ and $CH_2=CH^+$ respectively. These fragments can be attributed to 2-chloropropane ($(CH_3)_2CHCl$) [33] formed in-situ by eq. (4). Moreover, at 140 °C, the **A63E1** sample exhibited a new fragment at the m/z ratio= 148, while the **A36E1** sample showed two new fragments at the m/z ratios = 148 and 105 (marked by ○), in addition, the relative intensity at the m/z ratio = 133 became highest (marked by ○). The m/z ratios = 148, 133, and 105 are assigned as $(H_3C)_2C_6H_3\text{-}CH(CH_3)_2^+$, $H_3C\text{-}C_6H_3\text{-}CH(CH_3)_2^+$ and $(H_3C)_2C_6H_3^+$, respectively, and these fragments were attributed to dimethylcumene ($(H_3C)_2C_6H_3\text{-}CH(CH_3)_2$) formed in-situ by eq. (6).

It should be noted that the mass spectrum at 230 °C of the **A36E1** sample exhibited additional fragments at the m/z ratios = 101 and 99 ($SiHCl^{2+}$), 66 and 64 ($SiHCl^{+}$), 38 ($H^{37}Cl^{+}$), 36 ($H^{35}Cl^{+}$) and 17 (NH_3^{+}) (marked by ▼ in Fig. 3C). The evolution of NH_3 is due to the transamination reaction, which could be accelerated by the $AlCl_3$ as a Lewis acid catalyst. As suggested by the ATR-IR spectroscopic analysis, the excess $AlCl_3$ was coordinated with NH groups of PHPS, which could allow the Al-N bond formation via the nucleophilic attack of N of the NH groups to Al cation center of $AlCl_3$ followed by elimination of HCl. As another possible reaction, the released chloride anion (Cl^-) attacked other electrophiles such as the Si center of PHPS moieties to release chlorosilanes as previously discussed for chemical modification of PHPS with MCl_2 (M = Co [24], Ni [25]).

As shown in Fig. 3A–C, all the samples exhibited the third minor TICC peak at around 850 °C consisting mainly of fragments at the m/z ratios of 36 and 38 which can be assigned to HCl ($H^{35}Cl$, $H^{37}Cl$). As reported previously [19], the $EuCl_2$ remained without reacting with the residual alkoxide group, $(=N)_mAl(OR)_{3-m}$ up to approximately 744 °C, then began to melt accompanied by Cl^- elimination, which triggered the Eu-N bond formations with silylamino moiety derived from PHPS followed by elimination of HCl as a by-product (eq. (7)) [19].

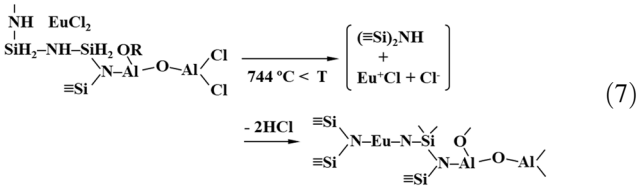

(7)

The chemical compositions of 1000 °C-pyrolyzed samples are listed in Table 2. The Al/Si and Eu/Si ratios of each sample are slightly higher than those of nominal ones calculated based on the composition listed in Table 1, which was due to the volatilization of low molecular fraction of as-received PHPS, monomeric chlorosilanes and oligomers formed in-situ during the chemical modification reactions. When pyrolysis was performed under flowing N_2, excess oxygen and residual carbon contents decreased consistently with the amount of $AlCl_3$ used for the chemical modification of PHPS. However, **NA36E1** sample showed higher Cl/Si ratio (0.10) compared with that of other samples (Cl/Si = 0.01~0.02). As discussed above, in this precursor (A36E1), unreacted $AlCl_3$ remained as stoichiometric excess for the NHSG reaction, which resulted in the higher amount of the residual Cl.

As shown in Table 2, compared with the NA63E1 sample, residual Cl content was reduced by the NH_3-pyrolysis, and the Cl/Si ratio of the NHA63E1 sample was measured to be 0.01. In addition, the C/Si ratio also decreased from 0.16 to 0.14. Accordingly, the combination of the NHSG reaction and subsequent FCA reaction during *single source* precursor synthesis and the NH_3-pyrolysis up to 1000 °C was effective to improve the purity of polymer-derived multicomponent SiAlEuON compound as an intermediate for synthesizing SiAlON:Eu^{2+} phosphors through the PDCs route.

3.3 Formation of β-SiAlON:Eu^{2+} phosphors

The 1000 °C-pyrolyzed samples were further heat-treated at 1800 °C under a N_2 pressure at 980 kPa. The chemical compositions of the 1800 °C-heat treated samples are listed in Table 3. Each sample was named by following that of the pyrolyzed sample, for instance, after the 1800 °C heat treatment, the NA63E1 sample was named 1800 °C-NA63E1. The z values were calculated by using the theoretical β-SiAlON formula, $Si_{6-z}Al_zO_{z-2y}N_{8-z+2y}$:$yEu^{2+}$ given by Wang et.al [3], and the chemical compositions were expressed as $Si_{6-z}Al_zO_{z-2y+\delta}N_{8-z+2y+\gamma}$:$yEu^{2+}$ as mentioned in the experimental section. The residual chlorine was successfully removed by the high-temperature heat treatment up to 1800 °C, and the resulting chlorine content in each sample was below the detection limit. Both the carbon and oxygen contents in each sample also apparently decreased, which suggests that, alongside the in-situ β-SiAlON formation, carbothermal reduction and subsequent nitridation reactions proceeded as reported for silica (SiO_2) in the presence of free carbon [19, 38].

XRD patterns of the heat-treated samples are shown in Fig. 4. All the samples show β-SiAlON single phase except

Table 2 Chemical compositions of 1000 °C-pyrolyzed samples

Precursor	Pyrolysis atmosphere	Pyrolyzed sample	EDS (molar ratio)			Element analysis (wt%)			Empirical formula
			Al/Si	Eu/Si	Cl/Si	O	N	C	
A90E1 [19]	N_2	**NA90E1**	0.11	0.02	0.02	5.70	22.25	6.25	$SiAl_{0.11}O_{0.19}N_{0.84}C_{0.28}Eu_{0.02}Cl_{0.02}$
A63E1	N_2	**NA63E1**	0.09	0.02	0.02	4.64	23.34	3.91	$SiAl_{0.09}O_{0.15}N_{0.84}C_{0.16}Eu_{0.02}Cl_{0.02}$
	NH_3	**NHA63E1**	0.11	0.02	0.01	3.99	30.51	3.01	$SiAl_{0.11}O_{0.14}N_{1.20}C_{0.14}Eu_{0.02}Cl_{0.01}$
A36E1	N_2	**NA36E1**	0.10	0.02	0.10	2.87	22.99	2.97	$SiAl_{0.10}O_{0.09}N_{0.86}C_{0.13}Eu_{0.02}Cl_{0.10}$

Table 3 Chemical compositions of 1800 °C-heated samples

Sample name	EDS (molar ratio)			Element analysis (wt %)			Chemical composition						β phase ratio (%)
	Al/Si	Eu/Si	Cl/Si[1)]	O	N	C	Empirical formula	$Si_{6-z}Al_zO_{z-2y+\delta}N_{8-z+2y+\gamma}$;$yEu^{2+}$			Eu^{2+} (mol%)		
								z	y	δ	γ		
1800 °C-NA90E1 [19]	0.10	0.01	*	2.33	34.37	1.80	$SiAl_{0.10}O_{0.07}N_{1.28}C_{0.08}Eu_{0.01}$	0.55	0.055	−0.05	−0.58	0.41	100
1800 °C-NA63E1	0.08	0.01	*	1.89	39.71	0.19	$SiAl_{0.08}O_{0.06}N_{1.53}C_{0.01}Eu_{0.01}$	0.44	0.056	0.00	0.83	0.37	100
1800 °C-NHA63E1	0.10	0.01	*	3.49	37.65	0.02	$SiAl_{0.10}O_{0.12}N_{1.49}C_{0.00}Eu_{0.01}$	0.55	0.055	0.22	0.56	0.37	100
1800 °C-NA36E1	0.06	(0.003)	*	2.03	37.35	0.45	$SiAl_{0.06}O_{0.06}N_{1.34}C_{0.02}Eu_{0.003}$	(0.34)[2)]	0.017	0.03	−0.11	0.12	84

1) *Cl content was below the detection limit

2) The z value was calculated as single phase β-SiAlON

the 1800 °C-NA36E1 sample which shows a mixture of α- and β-SiAlON phases.

The diffraction peak position of β-SiAlON shifts towards a lower diffraction angle consistently with the z value due to the lattice expansion by replacing the Si-N bond (0.174 nm) with the Al-O bond (0.175 nm) or Al-N bond (0.187 nm) [39, 40]. In this work, the shift was clearly observed at the 2θ corresponding to the strongest peak corresponding to the (101) plane of β-SiAlON as reported previously [40]: 33.666 (z = 0 (β-Si_3N_4), JCPDS card No. 33-1160), 33.525 (z = 0.44, 1800°C-NA63E1 sample) and 33.510 (z = 0.55, 1800 °C-NHA63E1 sample).

Funayama et al. reported that, in the case of high z values (z > 1), a mixture including impure J-SiAlON and mullite phases formed due to the excess oxygen originated from the chemical modifier of $Al(OR)_3$ [18]. In the present *single source* precursor synthesis, the total amount of Al-modifier was limited to control the z value as 0.5, and $Al(OR)_3$ was partly replaced by $AlCl_3$ to control the oxygen content while keeping the Al/Si molar ratio. Moreover, carbothermal reduction and subsequent nitridation efficiently proceeded during the 1800 °C-heat treatment, which lead to the successful formation of β-SiAlON:Eu^{2+} phosphors with chemical compositions close to the theoretical ones appropriate for z values. However, in the case of the **1800 °C-NA36E1** sample, a considerable amount of aluminum (Al) was also lost, which was due to the high amount of chlorine contamination at the amorphous state after the 1000 °C-pyrolysis in N_2 (Cl/Si=1.0, Table 2). This could lead to the limited amount of the transient liquid phase formed in-situ during the heat treatment, which resulted in the formation of a mixture of α- and β-SiAlON phases. Moreover, the morphology of the **1800 °C-NA36E1** was also different from those of other samples as shown in Fig. 5: the 1800 °C-heat treated samples exhibited typical rod-like β-SiAlON grains except **1800 °C-NA36E1** sample which was composed of a mixture of α- and β-SiAlON phases having rather equiaxed grains (Fig. 5(c)).

3.4 PL properties of polymer-derived β-SiAlON:Eu^{2+} phosphors

The room temperature PL excitation and emission spectra of the polymer-derived β-SiAlON:Eu^{2+} phosphor samples are shown in Fig. 6. The excitation spectra (Fig. 6(a)) were monitored at the appropriate maximum emission wavelengths of each sample shown in Fig. 6(c). The emission spectra shown in Fig. 6(b, c) were monitored under excitation at 410 and 460 nm, respectively. These polymer-derived phosphor samples exhibited a similar

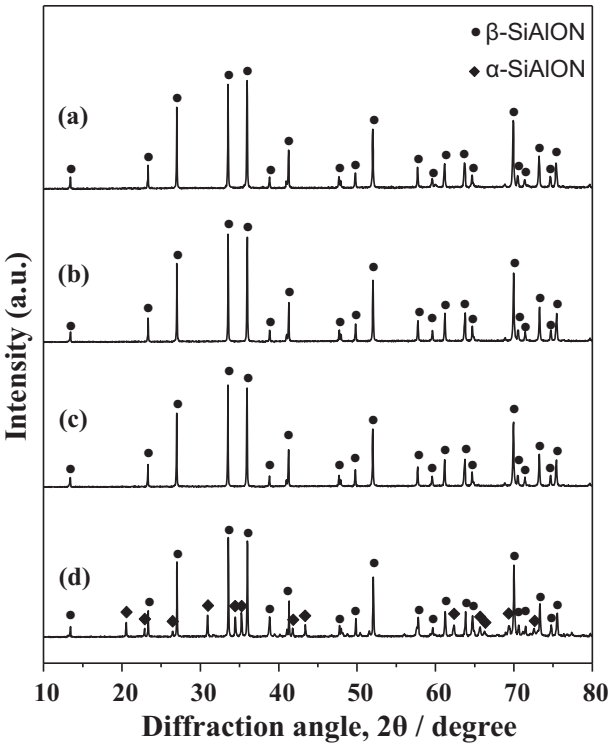

Fig. 4 XRD patterns polymer-derived β-SiAlON:Eu^{2+} phosphors. a **1800 °C-NA90E1** [19]. **b 1800 °C-NA63E1. c 1800 °C-NHA63E1**. **d 1800 °C-NA36E1** samples

excitation spectrum with a broad peak centered around 300 nm and several peaks around 410 to 500 nm attributed to the absorptions of host lattice and the $4f^7$-$4f^65d^1$ transitions of dopant Eu^{2+} cations, respectively [4], and exhibited a typical green emission under violet light excitation ($\lambda_{ex} = 410$ nm, Fig. 6(b)) or blue light excitation ($\lambda_{ex} = 460$ nm, Fig. 6(c)).

The PL excitation and emission spectra observed for the present polymer-derived β-SiAlON:Eu^{2+} phosphor samples were similar to those previously reported for the SiAlON:Eu^{2+} phosphors fabricated by the conventional powder metallurgy method [4–6]. Accordingly, it was suggested that the dopant Eu^{2+} ions in the host β-SiAlON were located interstitially within the channels of the six-membered ring along the *c* axis as previously reported by Kimoto et al. [41].

The emission peak intensity depends on the chemical composition as well as the phase purity of the phosphors: **1800°C-NA63E1** and **1800°C-NA90E1** [19] samples with a single β-SiAlON phase show obvious higher emission intensity than that of **1800°C-NA36E1** sample with α-SiAlON impurity. In addition, the green emission intensity ($\lambda_{ex} = 410$ nm) was found to be increased by reducing the carbon and chlorine impurities through the polymer-derived ceramics route investigated in this study, and the highest green emission intensity was achieved for the 1800 °C-NA63E1 sample. The mechanisms are now studied and will be clarified in near future.

4 Conclusions

In this work, a series of β-SiAlON:Eu^{2+} phosphors were synthesized through the PDCs route: high-purity *single source* precursors in which strictly controlled chemical composition was established at the molecular scale by chemical modification of a commercially available PHPS with $Al(OCH(CH_3)_2)_3$, $AlCl_3$ and $EuCl_2$. The *single source* precursors were successfully converted to β-SiAlON:Eu^{2+} phosphors by pyrolysis at 1000 °C under flowing N_2 or NH_3 followed by heat treatment at 1800 °C under a N_2 gas pressure at 980 kPa. The findings of our present study are summarized as follows:

1. In addition to the Al-N bond formation with PHPS, $AlCl_3$ reacted with $(\equiv Si)_{3-x}N(Al\text{-}OCH(CH_3)_2)_x$ ($x = 1, 2$) groups to release 2-chloropropane, which was analogous to the well-known non-hydrolytic sol-gel (NHSG) reaction between metal alkoxide and metal chloride. Subsequently, $AlCl_3$ acted as a Lewis acid catalyst to promote the Friedel-Craft alkylation (FCA) between xylene used as solvent and 2-chloropropane formed in-situ to afford dimethylcumene.
2. $EuCl_2$ remained without reacting with the residual alkoxide groups, $(=N)_mAl(OR)_{3-m}$ up to approximately 744 °C, then began to react with silylamino moiety derived from PHPS to afford Eu-N bonds associated with the elimination of HCl.
3. The oxygen content of the polymer-derived multicomponent SiAlEuON compound was finely controlled by selecting the $Al(OCH(CH_3)_2)_3/AlCl_3$ molar ratio in the *single source* precursor synthesis.
4. The NHSG reaction and subsequent FCA during the *single source* precursor synthesis and the NH_3-pyrolysis up to 1000 °C synergistically contributed to reducing the carbon and chlorine impurities of the polymer-derived multicomponent SiAlEuON compound.
5. β-SiAlON:Eu^{2+} phosphors with chemical compositions close to the theoretical ones expressed as $Si_{6-z}Al_zO_{z-2y}N_{8-z+2y}$:$yEu^{2+}$, and the z values and Eu^{2+} contents were found in the ranges of 0.44-0.55 and 0.37-0.41 at%, respectively.
6. The polymer-derived β-SiAlON:Eu^{2+} phosphors exhibited green emission under violet light (410 nm) or blue light (460 nm) excitation attributed to the $4f^7$-$4f^6(^7f_3)5d^1$ transition of dopant Eu^{2+} ions, and

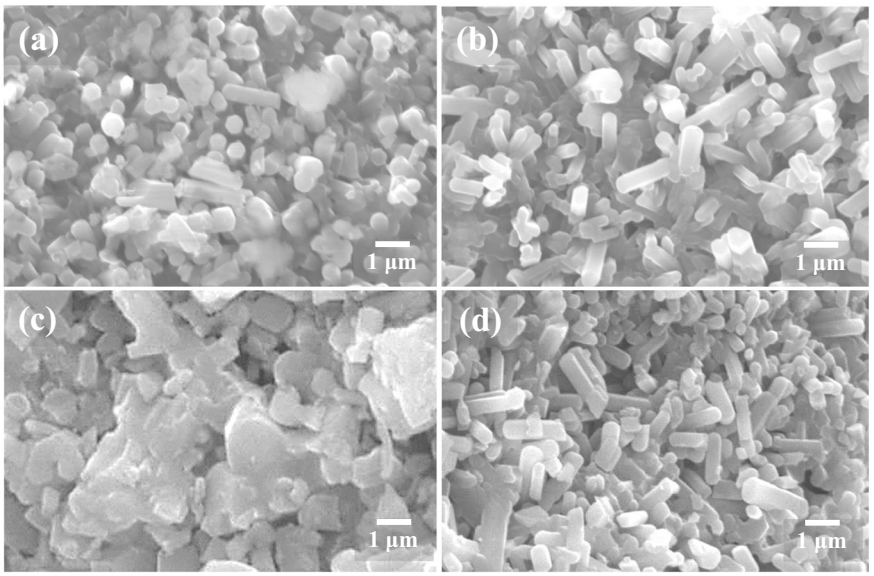

Fig. 5 SEM images showing morphology of polymer-derived β-SiAlON:Eu^{2+} phosphors. (**a**) **1800 °C-NA90E1** [19], (**b**) **1800 °C-NA63E1**, (**c**) **1800 °C-NA36E1** and (**d**) **1800 °C-NHA63E1** samples

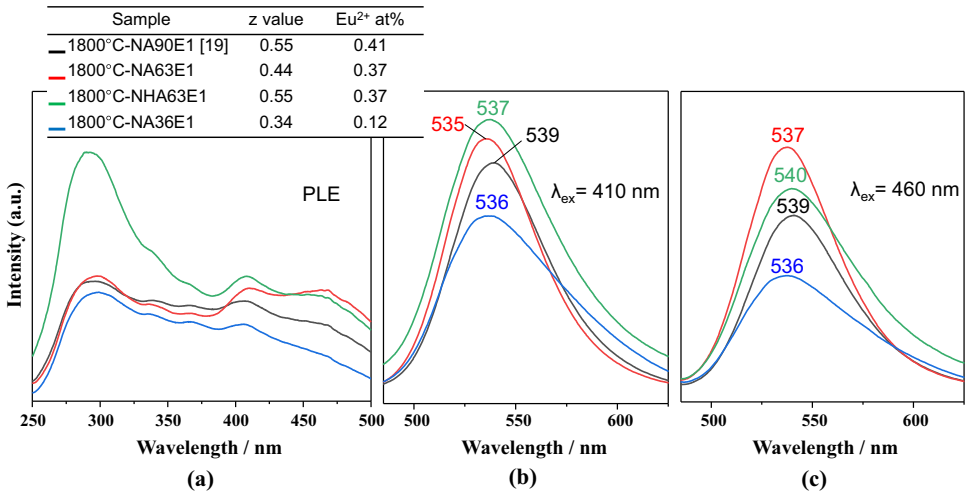

Fig. 6 **a** Excitation. **b**, **c** Emission spectra of polymer-derived β-SiAlON:Eu^{2+} phosphors

reduction of C and Cl impurities was found to be effective to improve the green emission properties of the polymer-derived β-SiAlON:Eu^{2+} phosphors.

Acknowledgements Dr. Samuel Bernard, Dr. Philippe Thomas and Prof. Yuji Iwamoto would like to thank CNRS who financially supported the present work via the International Research Project (IRP) 'Ceramics materials for societal challenges'. Mr. Daiki Hamana, Mr. Ryo Iwasaki, and Mr. Junya Iihama would like to thank the Nagoya Institute of Technology (NITech) who financially supported their present research work via the 'NITech for Global Initiative Projects'.

Author contributions All authors contributed to the study conception and design. YG conceived and planned this study, and drafted the manuscript; YG, DH, RI, JI, and MK contributed to the evaluation of samples; SH and TH contributed to Formal analysis; PT and SB reviewed the draft; Yuji Iwamoto conceived, reviewed, and supervised this work. The first draft of the manuscript was written by YG and all authors commented on previous versions of the manuscript. All authors read and approved the final manuscript.

Funding This work was supported by Japan Science and Technology Agency (JST) SPRING, Grant Number JPMJSP 2112.

Compliance with ethical standards

Conflict of interest The authors declare no competing interests.

Publisher's note Springer Nature remains neutral with regard to jurisdictional claims in published maps and institutional affiliations.

References

1. Zhang C, Uchikoshi T, Xie RJ, Liu L, Sakka Y, Hirosaki N (2019) Significantly improved photoluminescence of the green-emitting

β-sialon: Eu^{2+} phosphor via surface coating of TiO_2. J Am Ceram Soc 102:294–302. https://doi.org/10.1111/jace.15909
2. Xie RJ, Hirosaki N (2007) Silicon-based oxynitride and nitride phosphors for white LEDs-A review. Sci Technol Adv Mater 8:588–600. https://doi.org/10.1016/j.stam.2007.08.005
3. Wang Z, Ye W, Chu IH, Ong SP (2016) Elucidating structure–composition–property relationships of the β-SiAlON: Eu^{2+} Phosphor. Chem Mater 28:8622–8630. https://doi.org/10.1021/acs.chemmater.6b03555
4. Xie RJ, Hirosaki N, Li HL, Li YQ, Mitomo M (2007) Synthesis and photoluminescence properties of β-sialon: Eu2+(Si6−zAlzOzN8−z:Eu2+: A promising green oxynitride phosphor for white light-emitting diodes. J Electrochem Soc 154:J314–J319 https://doi.org/10.1149/1.2768289
5. Takahashi K, Xie RJ, Hirosaki N (2011) Toward higher color purity and narrower emission band β-sialon: Eu^{2+} by reducing the oxygen concentration. ECS Solid State Lett 14:E38-E40. https://doi.org/10.1149/2.017111esl
6. Li S, Wang L, Tang DM, Cho YJ, Liu XJ, Zhou XT, Lu L, Zhang L, Takeda T, Hirosaki N, Xie RJ (2018) Achieving high quantum efficiency narrow-band β-Sialon:Eu^{2+} phosphors for high-brightness LCD backlights by reducing the Eu^{3+} luminescence killer. Chem Mater 30:494-505. https://doi.org/10.1021/acs.chemmater.7b04605
7. Clément S, Mehdi A (2020) Sol-Gel chemistry: From molecule to functional materials. Molecules 25:2538. https://doi.org/10.3390/molecules25112538
8. Sanchez C, Boissiere C, Cassaignon S, Chanéac C, Durupthy O, Faustini M, Grosso D, Laberty-Robert C, Nicole L, Portehault D, Ribot F, Rozes L, Sassoye C (2014) Molecular engineering of functional inorganic and hybrid materials. Chem Mater 26:221–238. https://doi.org/10.1021/cm402528b
9. Sanchez C, Rozes L, Ribot F, Laberty-Robert C, Grosso D, Sassoye C, Boissiere C, Nicole L (2010) "Chimie douce": A land of opportunities for the designed construction of functional inorganic and hybrid organic-inorganic nanomaterials. C R Chim 13:3–39. https://doi.org/10.1016/j.crci.2009.06.001
10. Lale A, Schmidt M, Mallmann MD, Bezerra AVA, Acosta ED, Machado RAF, Demirci UB, Bernard S (2018) Polymer-Derived Ceramics with engineered mesoporosity: From design to application in catalysis. Surf Coat Technol 350:569–586. https://doi.org/10.1016/j.surfcoat.2018.07.061
11. Colombo P, Mera G, Riedel R, Soraru GD (2010) Polymer-derived ceramics: 40 years of research and innovation in advanced ceramics. J Am Ceram Soc 93:1805–1837. https://doi.org/10.1111/j.1551-2916.2010.03876.x
12. Ionescu E, Kleebe HJ, Riedel R (2012) Silicon-containing polymer-derived ceramic nanocomposites (PDC-NCs): preparative approaches and properties. Chem Soc Rev 41:5032–5052. https://doi.org/10.1039/C2CS15319J
13. Iwamoto Y, Ionescu E, Bernard S (2021) Preceramic Polymers as Precursors of Advanced Ceramics: The Polymer-Derived Ceramics (PDCs) Route. In: Hampshire S, Leriche A (ed.) Encyclopedia of materials: Technical ceramics and glasses. Elsevier, Amsterdam.
14. Funayama O, Arai M, Tashiro Y, Aoki H, Suzuki T, Tamura K, Kaya H, Nishii H, Isoda T (1990) Tensile strength of silicon nitride fibers produced from perhydropolysilazane. J Ceram Soc JAPAN 98:104–107. https://doi.org/10.2109/jcersj.98.104
15. Blanchard CR, Schwab ST (1994) X-ray diffraction analysis of the pyrolytic conversion of perhydropolysilazane into silicon nitride. J Am Ceram Soc 77:1729–1739. https://doi.org/10.1111/j.1151-2916.1994.tb07043.x
16. Iwamoto Y, Völger W, Kroke E, Riedel R, Saitou T, Matsunaga K (2001) Crystallization behavior of amorphous silicon carbonitride ceramics derived from organometallic precursors. J Am Ceram Soc 84:2170–2178. https://doi.org/10.1111/j.1151-2916.2001.tb00983.x
17. Funayama O, Kato T, Tashiro Y, Isoda T (1993) Synthesis of a polyborosilazane and its conversion into inorganic compounds. J Am Ceram Soc 76:717–723. https://doi.org/10.1111/j.1151-2916.1993.tb03665.x
18. Funayama O, Tashiro Y, Aoki T, Isoda T (1994) Synthesis and pyrolysis of polyaluminosilazane. J Ceram Soc JAPAN 102:908–912. https://doi.org/10.2109/jcersj.102.908
19. Gao Y, Iwasaki R, Hamana D, Iihama J, Honda S, Kumari M, Hayakawa T, Bernard S, Thomas P, Iwamoto Y (2022) Green emitting β-SiAlON:Eu^{2+} phosphors derived from chemically modified perhydropolysilazanes. Int J Appl Ceram Technol. (under review)
20. Iwamoto Y, Matsubara H, Brook R (1995) Microstructure development of Si_3N_4 ceramics derived from polymer precursor. In: Hausner H, Messing GL, Hirano S (ed.) Ceramic Processing Science and Technology, The American Ceramic Society, Westerville.
21. Iwamoto Y, Kikuta K, Hirano S (1998) Microstructural development of Si_3N_4–SiC–Y_2O_3 ceramics derived from polymeric precursors. J Mater Res 13:353–361. https://doi.org/10.1557/JMR.1998.0047
22. Iwamoto Y, Kikuta K, Hirano S (1999) Si_3N_4–SiC–Y_2O_3 ceramics derived from yttrium-modified block copolymer of perhydropolysilazane and hydroxy-polycarbosilane. J Mater Res 14:1886–1895. https://doi.org/10.1557/JMR.1999.0253
23. Iwamoto Y, Kikuta K, Hirano S (1999) Si_3N_4–TiN–Y_2O_3 ceramics derived from chemically modified perhydropolysilazane. J Mater Res 14:4294–4301. https://doi.org/10.1557/JMR.1999.0582
24. Tada S, Mallmann MD, Takagi H, Iihama J, Asakuma N, Asaka T, Daiko Y, Honda S, Nishihora RK, Machado RAF, Bernard S, Iwamoto Y (2021) Low temperature in situ formation of cobalt in silicon nitride toward functional nitride nanocomposites. Chem Commun 16:2057–2060. https://doi.org/10.1039/D0CC07366K
25. Asakuma N, Tada S, Kawaguchi E, Terashima M, Honda S, Nshihora RK, Carles P, Bernard S, Iwamoto Y (2022) Mechanistic investigation of the formation of nickel nano-crystallites embedded in amorphous silicon nitride nanocomposites. Nanomaterials 12:1644. https://doi.org/10.3390/nano12101644
26. Iwamoto Y, Kikuta K, Hirano S (2000) Synthesis of polytitanosilazanes and conversion into Si_3N_4-TiN ceramics. J Ceram Soc JAPAN 108:350–356. https://doi.org/10.2109/jcersj.108.1256_350
27. Iwamoto Y, Kikuta K, Hirano S (2000) Crystallization and microstructure development of Si_3N_4-Ti(C, N)-Y_2O_3 ceramics derived from chemically modified perhydropolysilazane. J Ceram Soc JAPAN 108:1072–1078. https://doi.org/10.2109/jcersj.108.1264_1072
28. Lale A, Mallmann MD, Tada S, Bruma A, Özkar S, Kumar R, Haneda M, Machado RAF, Iwamoto Y, Demirci UB, Bernard S (2020) Highly active, robust and reusable micro-/mesoporous TiN/Si_3N_4 nanocomposite-based catalysts for clean energy: Understanding the key role of TiN nanoclusters and amorphous Si_3N_4 matrix in the performance of the catalyst system. Appl Catal B 272:118975. https://doi.org/10.1016/j.apcatb.2020.118975
29. Funayama O, Aoki T, Isoda T (1996) Synthesis and pyrolysis of polyborosilazane with low oxygen content. J Ceram Soc JAPAN 104:355–360. https://doi.org/10.2109/jcersj.104.355
30. Gazzara CP, Messier DR (1977) Determination of phase content of Si_3N_4 by X-Ray diffraction analysis. Ceram Bull 56:777–780. https://bulletin-archive.ceramics.org/1977-09/
31. Christensen PA, Mashhadani ZTAW, Abd Halim Bin Md Ali, Carroll MA, Martin PA (2018) The production of methane, acetone, "Cold" CO and oxygenated species from isopropyl

alcohol in a Non-thermal plasma: An in-situ FTIR study. J Phys Chem A 122:4273–4284. https://doi.org/10.1021/acs.jpca.7b12297
32. Park SY, Kim N, Kim UY, Hong SI, Sasabe H (1990) Plasma polymerization of hexamethyldisilazane. Polym J 22:242–249. https://doi.org/10.1295/polymj.22.242
33. NIST Chemistry WebBook - SRD 69 (2017) National Institute of Standards and Technology, Gaithersburg. https://webbook.nist.gov/chemistry. Accessed 23 May 2022.
34. Vioux A, Mutin PH (2018) In: Klein L, Aparicio M, Jitianu A (ed) Handbook of Sol-Gel Science and Technology, Springe Nature Group, Berlin. https://doi.org/10.1007/978-3-319-32101-1
35. Acosta S, Corriu RJP, Leclercq D, Lefèvre P, Mutin PH, Vioux A (1994) Preparation of alumina gels by a non-hydrolytic sol-gel processing method. J Non Cryst Solids 170:234–242. https://doi.org/10.1016/0022-3093(94)90052-3
36. Vioux A (1997) Nonhydrolytic sol-gel routes to oxides. Chem Mater 9:2292–2299. https://doi.org/10.1021/cm970322a
37. Whalley P (2016) The comparison of Friedel-Crafts alkylation and acylation as a means to synthesise alkyl xylenes. The Plymouth Student. Scientist 9:252–296. http://hdl.handle.net/10026.1/14124
38. Weimer AW, Eisman GA, Sunsnitzky DW, Beaman DR, McCoy JW (1997) Mechanism and kinetics of the carbothermal nitridation synthesis of α-Silicon Nitride. J Am Ceram Soc 80:2853–2863. https://doi.org/10.1111/j.1151-2916.1997.tb03203.x
39. Ekström T, Nygren M (1992) SiAlON Ceramics. J Am Ceram Soc 75:259–276. https://doi.org/10.1111/j.1151-2916.1992.tb08175.x
40. Zhou Y, Yoshizawa Y, Hirao K, Lenčéš Z, Šajgalik P (2008) Preparation of Eu-doped β-SiAlON phosphors by combustion synthesis. J Am Ceram Soc 91:3082–3085. https://doi.org/10.1111/j.1551-2916.2008.02531.x
41. Kimoto K, Xie RJ, Matsui Y, Ishizuka K, Hirosaki N (2009) Direct observation of single dopant atom in light-emitting phosphor of β-SiAlON:Eu^{2+}. Appl Phys Lett 94:041908. https://doi.org/10.1063/1.3076110